Inelastic collisions in molecular nitrogen at low temperature ($2 \leqslant T \leqslant 50$ K)

J. P. Fonfría and A. Ramos
Instituto de Estructura de la Materia, CSIC, Serrano 121, 28006 Madrid, Spain

F. Thibault
Laboratoire de Physique des Atomes, Lasers, Molécules et Surfaces, UMR-CNRS 6627, Université de Rennes I, Campus de Beaulieu, F-35042 Rennes Cedex, France

G. Tejeda, J. M. Fernández, and S. Montero[a)]
Instituto de Estructura de la Materia, CSIC, Serrano 121, 28006 Madrid, Spain

(Received 17 July 2007; accepted 21 August 2007; published online 3 October 2007)

Theory and experiment are combined in a novel approach aimed at establishing a set of two-body state-to-state rates for elementary processes $ij \rightarrow \ell m$ in low temperature N_2:N_2 collisions involving the rotational states i,j,ℓ,m. First, a set of 148 collision cross sections is calculated as a function of the collision energy at the converged close-coupled level via the MOLSCAT code, using a recent potential energy surface for N_2–N_2. Then, the corresponding rates for the range of $2 \leqslant T \leqslant 50$ K are derived from the cross sections. The link between theory and experiment, aimed at assessing the calculated rates, is a master equation which accounts for the time evolution of rotational populations in a reference volume of gas in terms of the collision rates. In the experiment, the evolution of rotational populations is measured by Raman spectroscopy in a tiny reference volume ($\approx 2 \times 10^{-3}$ mm^3) of N_2 traveling along the axis of a supersonic jet. The calculated collisional rates are assessed experimentally in the range of $4 \leqslant T \leqslant 35$ K by means of the master equation, and then are scaled by averaging over a large set of experimental data. The scaled rates account accurately for the evolution of the rotational populations measured in a wide range of conditions. Accuracy of 10% is estimated for the main scaled rates. © *2007 American Institute of Physics*.
[DOI: 10.1063/1.2784255]

I. INTRODUCTION

Energy transfer induced by binary intermolecular collisions at kinetic energy E is usually described by means of cross sections $\sigma(E)$, while energy transfer in a bath at kinetic temperature T_t is described by the corresponding rates $k(T_t)$.

The two-body state-to-state cross sections $\sigma_{ij \rightarrow \ell m}$ and their associated $k_{ij \rightarrow \ell m}$ rates discussed below quantify in detail the effect of molecular collisions in terms of elementary processes $ij \rightarrow \ell m$ involving precollisional (i,j) and postcollisional (ℓ,m) quantum states of both molecules.

The microscopic description of a number of physical phenomena of fundamental or applied interest relies on σ's or k's. Furthermore, since these quantities may be derived from first principles by means of scattering calculations, with results highly sensitive to the intermolecular potential energy surface (PES), calculated σ's and k's provide a way to assess the quality of the PES by comparing with high level calculations or with experiment.

While a wide range of transport and relaxation phenomena in gases has been formulated in terms of σ's,[1] remote probing of gas density by the broadening of spectral lines is usually discussed in terms of k's. The breakdown of equilibrium between degrees of freedom in rarefied gases like supersonically expanding media or planetary atmospheres including Earth's upper atmosphere can also be studied in some depth by the intermediate of the k's. Moreover, the transfer of energy by inelastic collisions, a problem of increasing importance in the physics and chemistry of the interstellar molecular medium, requires inelastic rates in the lower end of the thermal scale, usually below 50 K.

For the mentioned reasons, much theoretical and experimental work has been done along the last decades toward obtaining accurate state-to-state cross sections and rates. Nonetheless, the problem remains elusive. This is due, in part, to the limitations of the intermolecular PES's so far available for most systems, and in part to the lack of suited experimental methods for testing σ's or k's associated with a single elementary collisional process.

In the case of N_2 the experiments based on spectral line shapes and line broadening, or even those based on pump-probe processes in gas media above 77 K, only provide information about functions which depend on a large number of two-body rates. At room temperature and above this number becomes unmanageable. These large sets are usually reduced to a manageable size of one-body rates $k_{i \rightarrow \ell}$ by thermal averaging over the initial states of one of the colliding partners, summing up over its final states. This, however, implies a lost of information and may lead to a compensation of errors.[2]

Inelastic molecular collisions have been widely studied by spectroscopic methods and by theory. Raman line broadening coefficients have been measured for N_2 between 77 and 1500 K (Refs. 3–11) and have been interpreted in terms

[a)]Electronic mail: emsalvador@iem.cfmac.csic.es

of effective one-body rates in the frame of several simplified molecular scattering models and fitting laws. One-body rates for $N_2:N_2$ collisions in the $v=1$ vibrational state have been determined at room temperature by a pump-probe technique.[12] Effective one-body inelastic rates for $N_2:N_2$ collisions have been investigated experimentally at very low temperature ($3 \leqslant T \leqslant 16$ K) by means of the evolution of rotational populations and of the rotational-translational nonequilibrium along supersonic expansions in free jets.[13]

Two-body cross sections and reduced one-body rates for $N_2:N_2$ collisions have been derived from quantum calculations at different levels of theory[2,14,15] using the PES of van der Avoird *et al.* (vdA-PES).[17] In these works the cross sections from the infinite order sudden approximation and from the coupled state (CS) approximation have been compared with the more accurate converged close coupling (CC) calculation. The highly averaged one-body effective rotational excitation rates calculated in the CS approximation in the vibrational ground state at 300 K up to $\Delta J=10$ are in remarkable good agreement with the corresponding experimental quantities.[12] However, no two-body cross sections nor rates suited for the interpretation of low-temperature ($T<100$ K) experiments appear to have been reported so far for N_2.

In the present work we report a theoretical-experimental study at low temperature where a large set of two-body rates for $N_2:N_2$ collisions is calculated for $2 \leqslant T \leqslant 50$ K in the frame of the CC scattering treatment[18,19] using a modified version[20] of vdA-PES.[17] These rates are then assesed in the range of $4 \leqslant T \leqslant 35$ K by means of the evolution of rotational populations measured by Raman spectroscopy along several supersonic jets, and finally, the original set of CC-calculated rates is scaled by a simple function of temperature to fit a large set of experimental data.

II. CALCULATED CROSS SECTIONS AND RATE COEFFICIENTS

The $N_2:N_2$ two-body cross sections $\sigma_{ij\to\ell m}$ at total energies $E_T \leqslant 263$ cm^{-1}, which are relevant at temperatures up to 50 K, have been calculated with the MOLSCAT code.[19] The PES (Ref. 20) employed was expanded over 30 bispherical harmonics.[17] The coupled equations were solved by means of the hybrid log-derivative-Airy propagator of Alexander and Manolopoulos.[21] The propagation was carried out with the diabatic modified log-derivative method from a minimum intermolecular distance of 2.5 Å to an intermediate one of 12 Å, and with the Airy method up to a maximum of 24 Å.

The set of calculated cross sections includes most collisionally induced transitions in the domain of rotational quantum number $J=\{i,j,\ell,m\} \leqslant 7$ and energy gaps $\Delta/B = |i(i+1)+j(j+1)-\ell(\ell+1)-m(m+1)| \leqslant 70$, where $B = 1.989\,730$ cm^{-1} is the rotational constant of N_2. Both variants of N_2 have been considered: ortho-N_2 (oN_2), and para-N_2 (pN_2). The $oN_2:oN_2$ and $pN_2:pN_2$ collisions have been treated in the approach of indistinguishable molecules. A total of 148 different cross sections has been calculated: 36 for $oN_2:oN_2$, 21 for $pN_2:pN_2$, and 91 for $oN_2:pN_2$ collisions. A high resolution grid of 0.1 cm^{-1} energy step has been employed in the regions with large $d\sigma/dE$ gradients, increasing the step size for decreasing gradients. Grids of 949, 642, and 900 energy points were employed for the $oN_2:oN_2$, $pN_2:pN_2$, and $oN_2:pN_2$ collisions, respectively. A representative set of calculated cross sections is shown in Fig. 1.

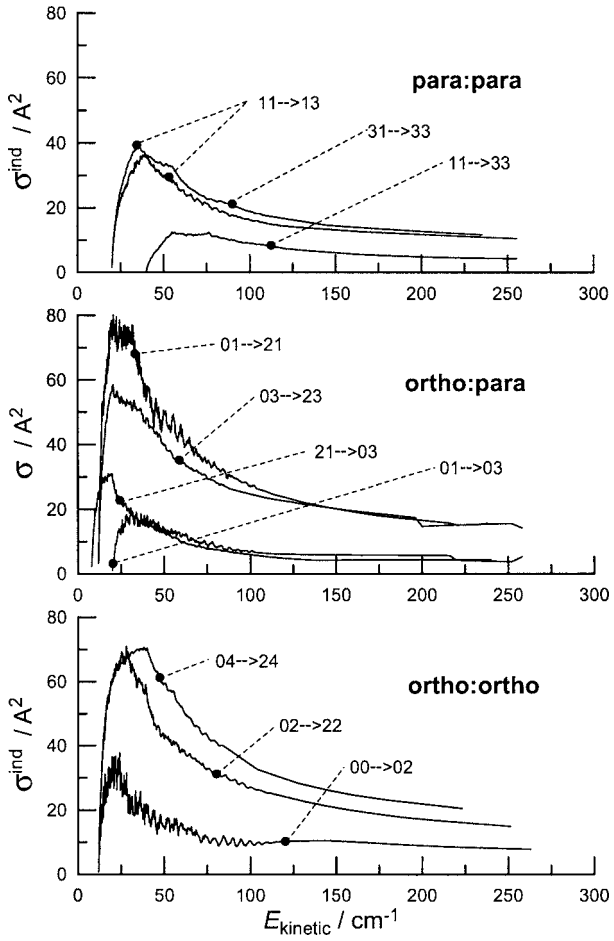

FIG. 1. CC-calculated cross sections for N_2.

Few inelastic cross sections for $N_2:N_2$ collisions have been reported so far at the highest level of theory. Some of the $oN_2:oN_2$ cross sections at total energies $E_T=119$ and 219 cm^{-1} calculated at the CC level of theory,[15] employing the original vdA-PES,[17] are shown in Table I jointly with the

TABLE I. CC-calculated cross sections (σ^+) (in Å^2) for $oN_2:oN_2$ collisions between indistinguishable molecules at total energies $E_T=119$ and 219 cm^{-1}. In parentheses, values from Ref. 15.

Process	119 cm^{-1}	219 cm^{-1}
$00\to40$	3.32 (2.55)	2.06 (1.88)
$00\to42$	10.82 (11.02)	6.08 (5.63)
$00\to44$	7.26 (4.98)	3.63 (3.60)
$02\to04$	8.67 (9.17)	5.31 (6.04)
$02\to42$	26.50 (26.39)	14.89 (14.89)
$02\to44$	9.49 (10.00)	6.36 (5.79)
$04\to42$	46.00 (34.08)	23.17 (18.61)
$04\to44$	16.89 (12.39)	8.23 (6.03)
$06\to40$	8.60 (10.04)	3.67 (3.72)
$06\to42$	36.18 (35.59)	12.21 (13.14)
$06\to44$	29.29 (23.39)	6.36 (5.16)

TABLE II. Spin weights for N_2-N_2.

Species	J	I	W^+	W^-
$oN_2:oN_2$	even	0	1	0
		2	3/5	2/5
$pN_2:pN_2$	odd	1	2/3	1/3

present results.

The statistic weights $W^+=(I+1)/(2I+1)$ and $W^-=I/(2I+1)$ of the symmetric and antisymmetric wave functions of N_2-N_2 due to the nuclear spin, $I=0,2$ for oN_2-oN_2 and $I=1$ for pN_2-pN_2, are summarized in Table II. The cross sections for indistinguishable molecules are

$$\sigma_{ij\to\ell m}^{\text{ind}} = W^+\sigma_{ij\to\ell m}^{+} + W^-\sigma_{ij\to\ell m}^{-}, \tag{1}$$

where σ^+ and σ^- are the cross sections for the symmetric and antisymmetric wave functions.[15] Collisions between indistinguishable molecules imply the same nuclear spin in both molecules. The cross sections for such collisions have been calculated with Takayanagi's scheme for counting of states.[22] Then, the result has been renormalized dividing by the factor $F=(1+\delta_{ij})(1+\delta_{\ell m})$ in order to correct for double counting, according to Ref. 15.

The following examples summarize the computational effort: a close coupling calculation for $pN_2:pN_2$ collisions of indistinguishable molecules at $E_T=100$ cm^{-1} performed on a basis of 11 "well ordered"[15] rotational levels [(1,1)–(9,3), five open and six closed], up to total angular momentum $J=100$, took 4 h CPU on a IBM Power 4 station for each σ^+ and σ^- cross sections. For the highest energy considered, $E_T=263$ cm^{-1}, and up to $J=130$, with a basis of 19 rotational levels [(1,1)–(13,1), 13 open and 6 closed] the CPU time was 133 h. For $oN_2:pN_2$ collisions the calculation becomes hardly affordable. At $E_T=263$ cm^{-1}, with 37 levels considered, 26 open and 11 closed, and $J=130$, the CPU time was 360 h per cross section. The homologous calculation requires only 6 h in the CS approximation which, however, is not too accurate in this range of energies.[15]

Present CC calculation confirms the trend $\sigma^+\approx\sigma^-$, especially at total energy above 100 cm^{-1}. Only for $00\to02$ the differences between σ^+ and σ^- are noticeable, with an oscillatory pattern as a function of energy. This, however, cannot be shown by the jet experiment, not even at the lowest thermal end since the rate coefficient, which is defined as

$$k_{ij\to\ell m}(T_t) = \frac{\langle v\rangle}{(k_B T_t)^2}\int_{E_s}^{\infty}\frac{\sigma_{ij\to\ell m}(E)}{\exp(E/k_B T_t)}EdE, \tag{2}$$

averages the cross section over a range of energies, always leading to a smooth dependence of the $k_{ij\to\ell m}$ rates on the temperature; $E=E_T-E_i-E_j$ is the available precollisional kinetic energy for the molecules in the $J=i$ and j rotational levels, E_s is the minimum kinetic energy for the levels $J=\ell$ and m to become accessible, and $\langle v\rangle=(8k_B T_t/\pi\mu)^{1/2}$ is the mean relative velocity of the colliding partners of reduced mass μ.

As may be inferred from Ref. 15, the cross sections of distinguishable and indistinguishable colliding molecules are related by[16]

$$\sigma_{ij\to\ell m}^{\text{ind}} = \sigma_{ij\to\ell m}^{d} + \sigma_{ij\to m\ell}^{e} + (W^+ - W^-)\sigma_{ij;\ell m}^{de}, \tag{3}$$

where $\sigma_{ij;\ell m}^{\text{de}}$ accounts for the quantum interference effects.

In order to test the consistency of the CC-calculated cross sections for indistinguishable molecules, the cross sections for distinguishable molecules in $oN_2:oN_2$ and $pN_2:pN_2$ collisions were recalculated using Eq. (3.10) of Ref. 15. To a very good approximation we obtained

$$\sigma^{\text{ind}} \approx \sigma^d + \sigma^e, \tag{4}$$

for all collisions considered, showing that the interference effects are negligible in the investigated range of energies.

The inelastic rates, henceforth referred to as CC rates, were obtained from the CC-calculated cross sections by means of Eq. (2). They are given in the auxiliar table N2RATES.TXT (Ref. 23) for $2\leqslant T_t\leqslant 50$ K. It must be stressed, however, that the reported set of rates is not complete enough to interpret experiments at temperatures above 35 K. Due to computational limitations some cross sections and rates, which are non-negligible at $T_t>35$ K, were not calculated.

III. EXPERIMENTAL METHODOLOGY

The experimental part of the methodology[13,24,25] relies on the properties of supersonic free jets and on the remarkable capabilities of Raman spectroscopy to measure accurately the local conditions along the jet.[26–28] The link between experiment (the axial region of the jet expansion) and theory (the calculated collisional rates of previous section) is provided by the master equation (MEQ),[29]

$$\frac{dP_i}{dt} = n\sum_{j,\ell\leqslant m}(-P_iP_jk_{ij\to\ell m} + P_\ell P_m k_{\ell m\to ij})Q_{ij\ell m}, \tag{5}$$

which describes the time evolution of the population P_i of a rotational state with quantum number $J=i$ as a consequence of inelastic collisions in a gas of diatomic molecules at instantaneous number density n and translational temperature T_t. In this work the k's are the two-body state-to-state rates accounting for the elementary collisional process,

$$N_2(i) + N_2(j) \xrightarrow{k_{ij\to\ell m}} N_2(\ell) + N_2(m), \tag{6}$$

between two N_2 molecules, one in the rotational state $J=i$ and the other in the rotational state $J=j$. As a consequence of the collision, the final states become $J=\ell$ and $J=m$. The collisional medium is a tiny parcel of gas at instantaneous distance z from the nozzle and translational temperature $T_t(z)$, traveling along the jet axis with supersonic flow velocity $V(z)=dz/dt$.

The particular case studied is natural N_2 in the vibrational ground state, a 2:1 mixture of orthonitrogen (oN_2) and paranitrogen (pN_2) with $J=even$ and $J=odd$, respectively. These variants of N_2 do not interconvert in the time scale of the supersonic expansion. The rotational populations in Eq. (5) are therefore normalized as

$$\sum_{i=\text{even}} P_i = 2/3, \quad \sum_{i=\text{odd}} P_i = 1/3. \tag{7}$$

In the MEQ [Eq. (5)] indistinguishable molecules are considered for $oN_2:oN_2$ and $pN_2:pN_2$ collisions and distinguishable molecules for $oN_2:pN_2$ collisions. The factor

$$Q_{ij\ell m} = [1 + \delta_{ij}(1 - \delta_{\ell i})(1 - \delta_{mi})][1 - \delta_{\ell i}(1 - \delta_{ij})] \times [1 - \delta_{mi}(1 - \delta_{ij})] \quad (8)$$

in the MEQ [Eq. (5)] accounts for the symmetry effects in collisions between indistinguishable molecules.[29]

The two-body rates obey the detailed balance

$$k_{\ell m \to ij} = k_{ij \to \ell m} \frac{(2i+1)(2j+1)}{(2\ell+1)(2m+1)} e^{(E_\ell + E_m - E_i - E_j)/k_B T_t}, \quad (9)$$

where E_i, E_j, E_ℓ, and E_m are the energies of the rotational levels involved. The upward ("up") and downward ("down") rates will henceforth be labeled as $k^{\text{up}}_{ij \to \ell m}$ and $k^{\text{down}}_{\ell m \to ij}$, respectively, under the constraint $E_i + E_j < E_\ell + E_m$.

Since up and down rate coefficients may differ at low temperature by many orders of magnitude, it is convenient to reformulate the MEQ [Eq. (5)] in terms of only down rates, which show a far smoother thermal dependence than the up rates. With aid of the Eq. (9), the MEQ [Eq. (5)] can then be rewritten in the general form,

$$dP_i/dt = \sum_{\tau\omega\sigma\rho} a_{\tau\omega\sigma\rho} k^{\text{down}}_{\tau\omega \to \sigma\rho}, \quad (10)$$

in terms of only down rates, i.e., with rotational energy $E_\tau + E_\omega > E_\sigma + E_\rho$. The indices τ, ω, σ, and ρ run over the values of the rotational quantum number J allowed by ortho-para nonconversion. At least one of these indices must be equal to i. Each $a_{\tau\omega\sigma\rho} k_{\tau\omega \to \sigma\rho}$ term in MEQ [Eq. (10)] accounts in a convenient factorized form (instantaneous local properties $\times$ intermolecular properties) for the net contribution of the $\sigma\rho \to \tau\omega$ and $\tau\omega \to \sigma\rho$ time-symmetric elementary collisional processes to the population rate dP_i/dt.

Coefficients $a_{\tau\omega\sigma\rho}$ are calculated with MEQNEW.FOR, an *ad hoc* FORTRAN code which uses the experimental data n, P_i, and T_t at a given point of the jet as input. If additionally, a set of $k^{\text{down}}_{\tau\omega \to \sigma\rho}$ rates is supplied in the data input, the code yields the individual contributions of the elementary collisions to the instantaneous rotational population rate dP_i/dt, i.e., the individual contributions to the right hand term (RHT) of the MEQ [Eq. (10)].

As discussed below, the population rates dP_i/dt for the rotational level $J=i$ in the left hand term (LHT) of the MEQ [Eq. (10)] as well as the quantities n, P_i, and T_t to calculate the $a_{\tau\omega\sigma\rho}$ coefficients with MEQNEW are determined directly from the experiment. In turn, the $k^{\text{down}}_{\tau\omega \to \sigma\rho}$ rates to be assessed by the experimental may originate from scattering calculations or from models.

The comparison between the experimental LHT's of the MEQ [Eq. (10)] for different rotational levels $J=i$ with the corresponding experimental-calculated RHT's by means of the code MEQNEW at different points of the supersonic jet provides a wealth of information about the quality of the collisional rates assessed. The procedure is described below in more detail.

IV. EXPERIMENT AND DATA REDUCTION

In order to test the internal consistency of the experimental data for a range of temperature-density conditions as wide as possible, four continuous free jets of N_2 at stagnation pressures of 200, 500, 1000, and 2000 mbars at room temperature have been measured. The jets were generated expanding the gas through a circular nozzle of diameter $D = 313$ μm into a $55 \times 44 \times 59$ cm^3 vacuum chamber especially devised for Raman spectroscopy measurements. Its vacuum system is based on a 1430 m^3/h Roots pump backed by a 70 m^3/h rotary pump.

The experimental quantities n, P_i, T_r, and T_t involved in the $a_{\tau\omega\sigma\rho}$ coefficients of MEQ [Eq. (10)], as well as dP_i/dt in its left-hand term, were determined at a number of points along the jet axis at distances z from the nozzle, as follows.

The number densities $n(z)$ were measured from the integrated Raman intensity of the Q branch of the vibrational band of N_2 at 2331 cm^{-1},

$$I^{\text{vib}}_{2331} = Kn(z), \quad (11)$$

which is strictly proportional to the number density of N_2 at the focal spot of the exciting laser beam for a very wide range of conditions. The constant K was determined using static N_2 as a standard in the sampling chamber, its pressure being measured with a MKS Baratron 690A of nominal accuracy of 0.08%.

The populations $P_i(z)$ were determined from the local intensities $I(z)$ of the spectral lines associated with the $i \to i+2$ rotational Raman transitions, which obey the relation

$$P_i(z) = GI(z) \frac{(2i+1)(2i+3)}{(i+1)(i+2)}. \quad (12)$$

The constant G is determined from the normalization condition $\Sigma_i P_i = 1$. Representative rotational Raman spectra recorded along the jet axis of one of the expansions are shown in Fig. 2.

The Boltzmann plots of the measured rotational populations P_i prove unambiguously that the vast majority of the molecules are accurately represented by a rotational temperature T_r, as stated before.[30] Just minor deviations from a Boltzmann distribution were observed at the lower end of observable densities.

The experimental data $n(z)$ and $T_r(z)$ can be represented accurately by the empirical functions

$$n(z) = \frac{C_1}{(z + C_2)^2}, \quad \text{for } z \geqslant 1250\ \mu\text{m}, \quad (13)$$

and

$$T_r = T^* - (T^* - T_\infty) e^{-C_3/(z+C_4)}, \quad \text{for } z \geqslant 300\ \mu\text{m}, \quad (14)$$

where $T^* = 250$ K is the critical temperature at the origin ($z=0$, Mach number $M=1$) of the expansion and T_∞ is the terminal rotational temperature. The upper limit of validity of Eqs. (13) and (14) is imposed by the normal shock wave of the jet, centered at $z \approx 22\,000$ μm for all four expansions, but with shock widths differing by about one order of magnitude. The parameters C_i characterizing the expansions are

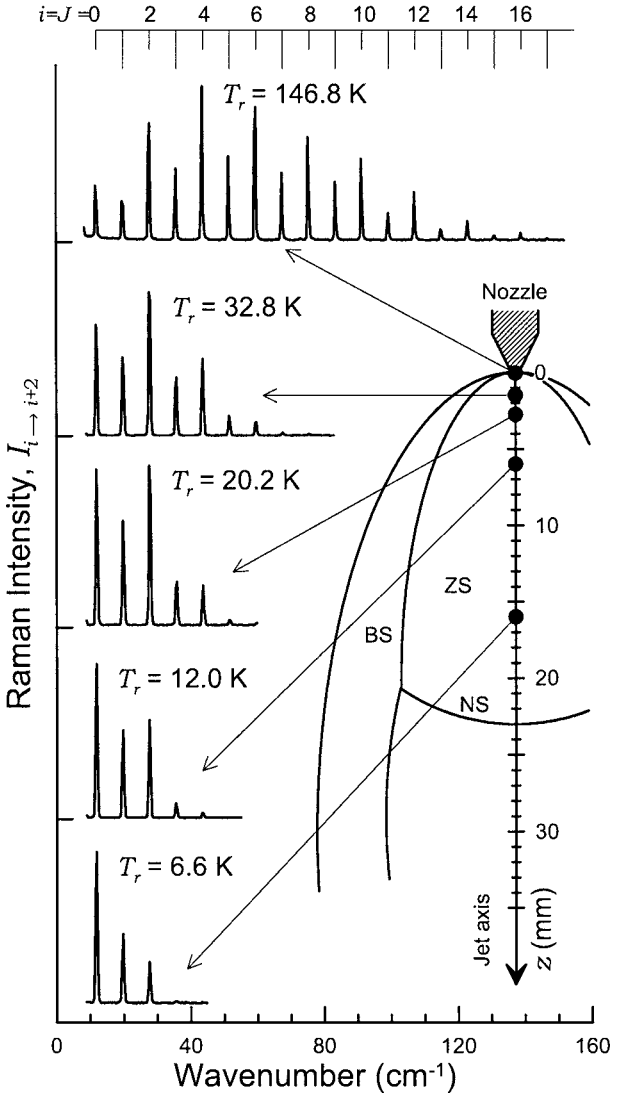

FIG. 2. Rotational Raman spectra of N_2 in a jet at p_0=2000 mbars; T_0: 297 K. ZS zone of silence; NS: normal shock; BS: barrel shock.

given in Table III for z expressed in μm in Eqs. (13) and (14). The uncertainty (one standard deviation) of the data retrieved from Eqs. (13) and (14) is less than 1% for n and $\approx$2% for T_r in all four expansions.

In the working region of the jet (zone of silence) the flow is laminar, and the distance z can be related with the time t elapsed from the beginning of the expansion (z=0) by means of the flow velocity $V(z)=dz/dt$. The population rates in the LHT of MEQ [Eq. (10)] are thus determined from

$$\frac{dP_i}{dt} = \frac{dP_i}{dz} V(z). \tag{15}$$

The quantities P_i, dP_i/dz and n employed to work through MEQ [Eq. (10)] were retrieved from Eqs. (13)–(15), since their accuracy is about one order of magnitude better than that of the individual raw data.

The flow velocity $V(z)$ in Eq. (15) was determined assuming the conservation of enthalpy along the expansion axis,[31] which leads to

$$V(z) = [R(7T_0 - 5T_t(z) - 2T_r(z))/W]^{1/2}, \tag{16}$$

where R=8.3145 J K^{-1} is the universal gas constant and W =0.028 kg/mol is the molar mass of N_2.

The translational temperatures $T_t(z)$ have been deduced in terms of the corresponding local number density and rotational temperature, and stagnation conditions, by means of

$$T_t(z) = T_0 \left(\frac{n(z)}{T_r(z)} \frac{T_0}{n_0} \right)^{2/3}. \tag{17}$$

This equation has been derived from the statistical definition of entropy employing a classical rotational partition function, under the assumption of entropy invariance along the axial flow line of the supersonic expansion. For N_2 the intrinsic accuracy of Eq. (17) is $\approx$2.5% at T_r=6.5 K and much better at higher temperatures. The accuracy of T_t depends on that of n, T_r, n_0, and T_0.

V. DISCUSSION

The CC rates, calculated according to Sec. II and listed in table N2RATES.TXT,[23] have been partially assessed by its capability to reproduce experimental values of dP_i/dt of MEQ [Eq. (10)] along the jets. These values have been measured at fixed points corresponding to kinetic temperatures T_t=35, 28, 22, 18, 14, 10, 8, 6, and 4 K. At these points, which approximately span along the jet the domain of $1250 \leqslant z \leqslant 14800$ μm, $40 \geqslant T_r \geqslant 7$ K, and $15\times10^{22} \geqslant n \geqslant 4\times10^{20}$ m^{-3}, the ratio,

$$R_i(T_t) = \frac{(\mathrm{LHT})_i}{(\mathrm{RHT})_i}, \tag{18}$$

of the left to the right-hand terms of MEQ [Eq. (10)] has been employed as an objective measure for the quality of the CC-calculated set of rates at temperature $T_t \leqslant 35$ K. While the $(\mathrm{LHT})_i$'s of MEQ [Eq. (10)] are purely experimental quantities, the $(\mathrm{RHT})_i$'s combine experimental quantities in the $a_{\tau\omega\sigma\rho}$ coefficients with the calculated, $k^{\mathrm{down}}_{\tau\omega\rightarrow\sigma\rho}$ CC rates.

TABLE III. Parameters characterizing the four supersonic jets of N_2 according to Eqs. (13) and (14); p_0, n_0, T_0 are the stagnation conditions.

p_0 (mbars)	n_0 (10^{22} m^{-3})	T_0 (K)	C_1 (10^{30} μm^2/m^3)	C_2 (μm)	T_∞ (K)	C_3 (μm)	C_4 (μm)
2000	4878	297	0.402	−50	4.030	199.020	113
1000	2439	297	0.210	−20	5.642	188.884	90
500	1228	295	0.118	40	7.852	187.589	140
200	491.1	295	0.043	0	13.000	165.197	90

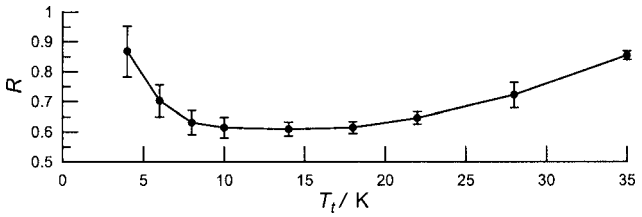

FIG. 3. Scaling function R=LHT/RHT.

The ratio R_i is best defined for $i=J=0,1$, the ground rotational levels of oN_2 and pN_2, since these dP_i/dt's are intrinsically positive along the supersonic expansion, as corresponding to a rotational cooling.

The statistics of the R_i ratios determined includes 62 data points from the four expansions. It reveals three important features.

(1) For a fixed T_t, the R_i ratio is nearly the same for all four expansions. This provides a strong evidence of the consistency of the experimental global data set $\{n, P_i, dP_i/dt, T_r, T_t\}$.
(2) The determined ratios are in the interval of $0.61 < R_i < 0.87$ in all cases, suggesting that the CC-calculated rates are too large by up to 64%, depending on T_t.
(3) For a fixed T_t, the R_i ratio is nearly independent on rotational quantum number $i=J=0,1,2,3$. This suggests that the CC-calculated rates, types $k_{0\omega\to\sigma\rho}$, $k_{1\omega\to\sigma\rho}$, $k_{2\omega\to\sigma\rho}$, and $k_{3\omega\to\sigma\rho}$, are off by about the same amount.

These trends are summarized in Fig. 3, where $R(T_t)$ is the average of R_i over $J=0$ and $J=1$ levels of the four expansions. The error bars refer to one standard deviation. They confirm that the combined effect of all experimental errors in n, P_i, T_r, and T_t over the four jets is typically less than 10%. This establishes the precision limit in assessing calculated rates by the present methodology, assuming that no systematic errors are hidden.

By virtue of (2) and (3) the $R(T_t)$ function of Fig. 3 is useful to scale the CC-calculated rates in order to produce experimentally scaled (ES) rates,

$$k^{\mathrm{ES}}_{\tau\omega\to\sigma\rho} = R(T_t) k^{\mathrm{CC}}_{\tau\omega\to\sigma\rho}, \tag{19}$$

fully compatible with the experimental information. The $k^{\mathrm{ES}}_{\tau\omega\to\sigma\rho}$ rates have the same relative values as the $k^{\mathrm{CC}}_{\tau\omega\to\sigma\rho}$ rates, and are thus determined by the close coupling calcula-

TABLE IV. Experimentally scaled rates (ES rates) for $J\leqslant 4$ rotational states in N_2:N_2 collisions at $35\geqslant T_t\geqslant 4$ K. Rates are in units of 10^{-20} m^3/s; energy gaps Δ in units of $B=1.989\,73$ cm^{-1}, the rotational constant of N_2. Indistinguishable molecules in ortho:ortho and para:para collisions.

Process	$\lvert\Delta\rvert$	T_t=35 K	28	22	18	14	10	8	6	4
03→21	4	8791	7815	7416	7348	7594	7913	8184	9029	10 674
41→23	4	7722	6739	6188	5943	5889	5791	5778	6126	6 970
20→00	6	1084	959	911	907	946	1003	1052	1182	1 436
21→01	6	3050	2653	2456	2390	2423	2471	2532	2780	3 313
22→02	6	2684	2346	2166	2094	2097	2099	2123	2292	2 679
23→03	6	2436	2086	1896	1822	1822	1836	1871	2043	2 413
24→04	6	3105	2671	2417	2275	2215	2150	2144	2294	2 673
40→22	8	6928	6167	5816	5748	5921	6148	6348	6988	8 229
30→10	10	1868	1663	1576	1553	1592	1642	1693	1872	2 244
31→11	10	3824	3333	3061	2942	2920	2886	2897	3113	3 645
32→12	10	4799	4141	3787	3648	3648	3666	3729	4067	4 826
33→13	10	4247	3705	3406	3281	3275	3234	3249	3482	4 027
34→14	10	3819	3237	2884	2724	2669	2632	2658	2889	3 427
41→03	10	1428	1258	1167	1127	1121	1099	1091	1146	1 282
22→00	12	289	250	229	219	217	215	218	235	278
40→20	14	3019	2645	2468	2417	2468	2543	2619	2880	3 401
41→21	14	3624	3180	2955	2867	2871	2855	2866	3060	3 512
42→22	14	4307	3726	3381	3214	3147	3066	3059	3269	3 800
43→23	14	4535	3907	3541	3378	3338	3315	3358	3654	4 332
44→24	14	4088	3520	3196	3054	3024	3002	3033	3281	3 854
23→01	16	932	803	732	703	701	702	712	774	911
40→00	20	257	227	213	208	211	216	221	241	279
41→01	20	652	568	521	499	493	480	475	496	548
42→02	20	1672	1450	1315	1248	1216	1175	1166	1239	1 434
43→03	20	914	780	694	651	630	608	605	645	739
44→04	20	746	651	599	577	575	569	572	614	709
33→11	20	889	772	704	671	659	642	637	672	764
43→21	24	1945	1680	1518	1440	1410	1382	1388	1495	2014
42→00	26	138	119	108	102	98	94	92	96	108
44→22	28	1083	936	851	812	801	790	791	848	979
43→01	30	383	326	288	268	257	246	244	260	300
44→02	34	417	361	329	314	311	305	307	330	385
44→00	40	52	45	41	39	38	37	38	41	49

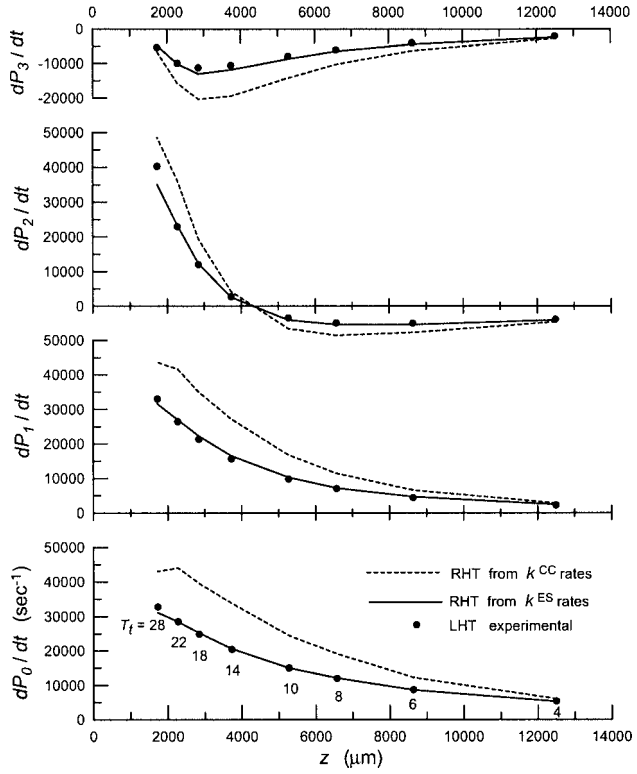

FIG. 4. RHT vs LHT of MEQ [Eq. (10)] for the expansion at p_0 =500 mbars. See the text.

tion, but their absolute values are determined by the experiment over a large data set. A selection of (down) $k^{\mathrm{ES}}_{\tau\omega\to\sigma\rho}$ rates for the collisionally induced transition between the $J\leqslant 4$ rotational levels of N_2 is given in Table IV. The corresponding up rates can be obtained from the detailed balance Eq. (9).

The set given in Table IV is sufficient to fully account for the dP_i/dt's at jet axial points where T_t=4 K. But at 35 K it only accounts for ≈60% of the dP_i/dt's since many other elementary processes involving $J\geqslant 5$ levels, not included in Table IV, are relevant at this temperature.

Accounting for 95% of the dP_i/dt's ($i=J\leqslant 3$) at 35 K requires a set of at least 148 $k^{\mathrm{ES}}_{\tau\omega\to\sigma\rho}$ rates. This set, which can be retrieved from table N2RATES.TXT (Ref. 23) multiplying by the factor $R(T_t)$, accounts for the experimental dP_i/dt's to good accuracy in all four jet expansions.

As an example, the rotational population rates dP_i/dt's along the N_2 jet generated at p_0=500 mbars are shown in Fig. 4. The full circles stand for the experimental LHT's of MEQ [Eq. (10)]. The dashed line represents the RHT of the MEQ [Eq. (10)] calculated with the set of 148 $k^{\mathrm{CC}}_{\tau\omega\to\sigma\rho}$ rates; the solid line stands for the RHT's calculated with the 148 $k^{\mathrm{ES}}_{\tau\omega\to\sigma\rho}$ rates. Note that this solid line *is not* a fit to the experimental data points shown, but arises from the average of the whole experimental data set from the four jets. The predictive ability of the $k^{\mathrm{ES}}_{\tau\omega\to\sigma\rho}$ rates for the other three jets, generated at p_0=200, 1000, and 2000 mbars, is about as good as in Fig. 4.

Although the accuracy of the individual $k^{\mathrm{ES}}_{\tau\omega\to\sigma\rho}$ rates of Table IV cannot be established from the experiment, the global accuracy of the subset with $\Delta\leqslant 16$ relevant to the thermal evolution of the $J\leqslant 4$ rotational levels is probably better than

TABLE V. Selection of close-coupled calculated rates (CC rates) vs experimentally scaled rates (ES rates) for N_2:N_2 collisions. Units of 10^{-20} m^3/s. Indistinguishable molecules in ortho:ortho and para:para collisions.

Process		T_t=35 K	T_t=18 K	T_t=4 K
03→21	CC rate	10 205	11 968	12 297
	ES rate	8 791	7 348	10 674
20→00	CC rate	1 260	1 477	1 655
	ES rate	1 084	907	1 436
21→01	CC rate	3 555	3 893	3 817
	ES rate	3 050	2 390	3 313
30→10	CC rate	2 169	2 530	2 585
	ES rate	1 868	1 553	2 244
31→11	CC rate	4 455	4 792	4 199
	ES rate	3 824	2 942	3 645
40→20	CC rate	3 514	3 937	3 918
	ES rate	3 019	2 417	3 401

10%. A selection of $k^{\mathrm{CC}}_{\tau\omega\to\sigma\rho}$ and $k^{\mathrm{ES}}_{\tau\omega\to\sigma\rho}$ rates at several temperatures is shown in Table V for comparison.

Two features of the rates in Table IV must be emphasized. First, and obvious, their smooth dependence on the kinetic temperature T_t. Second, and not obvious at all, the uncorrelated contribution of the rates to dP_i/dt. This is due to the multiplicative $a_{\tau\omega\sigma\rho}$ coefficients in MEQ [Eq. (10)]. Some large rates are multiplied by small $a_{\tau\omega\sigma\rho}$'s, and some small rates are multiplied by large $a_{\tau\omega\sigma\rho}$'s. Therefore it is not possible *a priori* to reduce the set of relevant rates. Only the calculation of the RHT of MEQ [Eq. (10)] with a sufficiently large set of rates permits us to decide about this point.

According to MEQ [Eq. (10)] the actual contribution of each elementary collisional process $\tau\omega\rightleftharpoons\sigma\rho$ to the evolution of the rotational populations at a given point of a jet is given by the individual contributions $a_{\tau\omega\sigma\rho}k_{\tau\omega\to\sigma\rho}$. Since the number of such contributions is very large as soon as the kinetic local temperature is above a few kelvins, a way to visualize them is by means of a collisional spectrum, a concept introduced in a previous work.[25] An example of collisional spectra is shown in Fig. 5. It accounts in full detail for the rotational thermal evolution by inelastic collisions at a given point of the jet. The bars indicate quantitatively the actual contribution of the elementary collisional processes to the global population rate of the ground rotational levels of oN_2 (dP_0/dt) and pN_2 (dP_1/dt). Each bar is a summand of the RHT of the MEQ [Eq. (10)]. The abscisa refers to the energy gaps Δ associated with the particular collisional process indicated. Note the assymmetry with respect to the origin, which shows that the system is evolving thermally. In this particular example, the sum of positive bars is larger than the sum of negative bars, indicates a tendency toward globally populating the ground rotational levels of oN_2 and pN_2, i.e., the rotational cooling occurring at a point of the zone of silence of the jet.

As indicated in the inset of Fig. 5, "UP" refers to collisionally induced transitions where the final rotational energy of the colliding couple is larger than the initial one, while

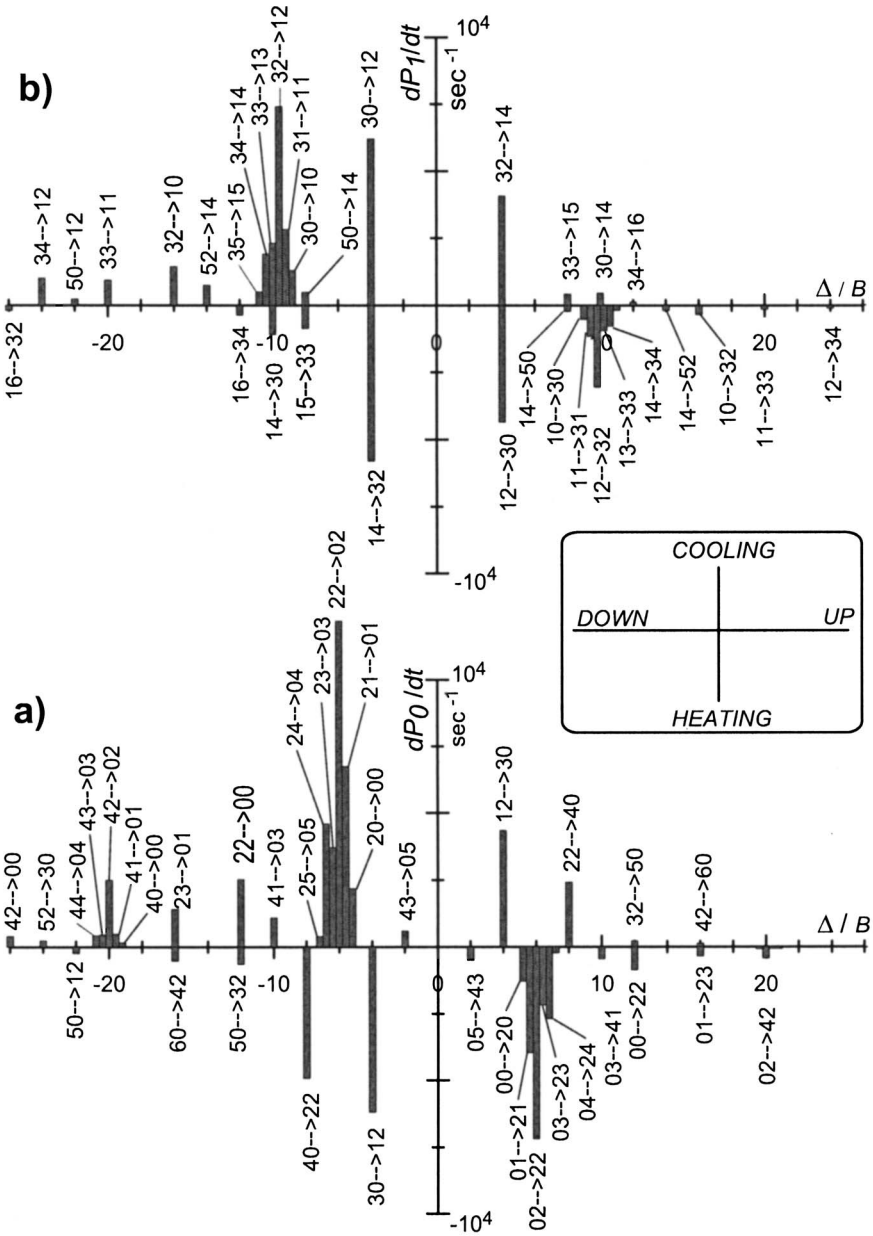

FIG. 5. Collisional spectra for the ground rotational levels of oN_2 (a) and pN_2 (b); point $z=2183$ μm of the jet generated at $p_0=200$ mbars, where $T_t=14$ K and $T_r=24.7$ K.

"DOWN" is the reversed process. Note that in some processes one molecule may go up and, simultaneously, the other goes down, like in $30\rightarrow 12$ at $\Delta=-4B$. Such simultaneous excitation-deexcitation processes are not negligible at all.

Positive bars (COOLING) are associated with the processes which tend to populate $(dP_i/dt>0)$ the ground rotational levels of ortho- and para-N_2. Negative bars (HEATING) describe the depopulation $(dP_i/dt<0)$ of the ground levels.

Collisional spectra alike to that in Fig. 5 can be obtained at every point of N_2 supersonic jets for a wide range of conditions by using the results of the present work. This allows tracking in detail the contribution of each collision channel to the evolution of rotational populations. Though the number of collisional channels is usually large, it can be noticed from Fig. 5 that only some of them are dominant, this effect being strongly dependent on the temperature.

VI. SUMMARY, CONCLUSIONS, AND FINAL REMARKS

Close coupling scattering calculations for N_2:N_2 collisions have been performed using the PES of Ref. 20. State-to-state cross sections have been calculated for 148 elementary $ij\rightarrow\ell m$ collisional processes involving rotational levels of N_2 up to $J=7$, in a grid of energies up to 263 cm^{-1}. This set of cross sections has been transformed into the corresponding state-to-state rate coefficients (CC rates) at temperatures in the range of $2\leqslant T_t\leqslant 50$ K. These CC rates have been assessed experimentally in the range of $4\leqslant T_t\leqslant 35$ K by means of the evolution of rotational populations measured by Raman spectroscopy along supersonic expansions of N_2. The CC rates systematically overestimate the experimental results by up to 64%, depending on temperature. With the aid of the experiment, the CC rates have been scaled by a simple function of $0.61<R(T_t)<0.87$. The scaled rates (ES rates) account for all experimental results, which span over a wide

range of thermal, density, and hydrodynamic conditions. In practical terms this provides the basis for the molecular explanation of supersonic flow evolution in terms of the elementary collisional processes. This is possible in full quantitative detail in the frame of a master equation which combines collisional rates with instantaneous number densities, rotational, and translational temperatures.

The following conclusions are drawn from present work.

(1) According to the experiment, the ES rates of Table IV for $\Delta \leqslant 16$ are accurate to $\approx 10\%$.
(2) The cross sections calculated here, and in a previous work[15] at the close coupling level, are somewhat different (see Table I). This may be attributed to the different PES's employed.[17,20]
(3) According to the experiment, the PES (Ref. 20) employed in the close coupling calculation needs to be improved in the region of the potential well.
(4) The experimental methodology (supersonic jet +Raman spectroscopy) proves highly efficient for assessing calculated state-to-state rate coefficients of molecular gases at temperatures well below the freezing point, a region hardly accessible to other techniques based on static gas samples.
(5) For $N_2:N_2$ collisions the current upper limit of present experimental method is $T_t \approx 50$ K. This limit might be extended toward higher temperature by using slit nozzles and softer stagnation pressures.
(6) The upper limit of the range assessed, $4 \leqslant T_t \leqslant 35$ K, is imposed by the accuracy of the current experimental data and by the limited number (148) of the calculated CC rates. At $T_t > 35$ K, the contribution from other rates which have not been calculated is increasingly important. This precludes a meaningful assessment of rates using experimental data up to 50 K.
(7) Collisional state-to-state rates derived from close coupling scattering calculations for $N_2:N_2$ at $T_t \geqslant 50$ K pose a serious computational challenge due to the larger range of energies required and to the fast increase of the number of relevant collisional processes with temperature. The coupled states approximation might be a good choice for testing with the present experimental method at $T_t \geqslant 50$ K.

The present experimental methodology is particularly well suited for studying inelastic collisional rates of molecules in the vibrational ground state. A generalization to vibrationally excited states appears feasible in the light of experimental developments capable of providing sufficient density of molecules in selected vibrational excited states by means of stimulated Raman pumping.[32] This is an instrumental possibility worthwhile to be explored.

Although the present work is aimed at the concrete problem of validating the rate coefficients for $N_2:N_2$ inelastic collisions at low temperature, it should be noted that the range of kinetic temperatures in this experiment, $4 \leqslant T_t \leqslant 35$ K, bridges the domain between the usual chemistry regime and that of cold diluted molecular systems. This is a fast growing field of research[33] where the possibility of controlling the collision dynamics by means of external fields opens exciting instrumental options.[34] Whether this sort of control can be implemented in the present methodology, which is also amenable to polar molecules, is a laboratory task for the future.

ACKNOWLEDGMENTS

This work has been supported by the Spanish Ministerio de Educación y Ciencia, research Project Nos. FIS2004-02576, HF2004-232, ESP2004-21060-E, and ASTROCAM network. J.P.F. is indebted to the CSIC for an I3P grant.

[1] F. R. W. McCourt, J. J. M. Beenakker, W. E. Köhler, and I. Kuscer, *Nonequilibrium Phenomena in Polyatomic Gases* (Clarendon, Oxford, 1991).
[2] S. Green, J. Chem. Phys. **98**, 257 (1993); **99**, 4875(E) (1993).
[3] L. Gómez, thesis, Universidad Computense de Madrid/Université de Franche Comté, 2007.
[4] L. Gómez, R. Z. Martínez, D. Bermejo, F. Thibault, P. Joubert, B. Bussery-Honvault, and J. Bonamy, J. Chem. Phys. **126**, 204302 (2007).
[5] G. C. Herring and B. W. South, J. Quant. Spectrosc. Radiat. Transf. **52**, 835 (1994).
[6] G. J. Rosasco, W. Lempert, and W. S. Hurst, Chem. Phys. Lett. **97**, 435 (1983).
[7] L. A. Rahn and R. E. Palmer, J. Opt. Soc. Am. B **9**, 1164 (1986).
[8] B. Lavorel, G. Millot, R. Saint-Loup, C. Wenger, H. Berger, J. P. Sala, J. Bonamy, and D. Robert, J. Phys. (Paris) **47**, 417 (1986).
[9] M. L. Koszykowski, L. A. Rahn, R. E. Palmer, and M. E. Coltrin, J. Phys. Chem. **91**, 41 (1987).
[10] L. Bonamy, J. Bonamy, D. Robert, B. Lavorel, R. Saint-Loup, R. Chaux, J. Santos, and H. Berger, J. Chem. Phys. **89**, 5568 (1988).
[11] R. G. Sharafutdinov, A. E. Belikov, M. L. Strekalov, and A. V. Storozhev, Chem. Phys. **207**, 193 (1996).
[12] G. O. Sitz and R. L. Farrow, J. Chem. Phys. **93**, 7883 (1990).
[13] A. Ramos, G. Tejeda, J. M. Fernández, and S. Montero, Phys. Rev. A **66**, 022702 (2002).
[14] S. Green and W. M. Huo, J. Chem. Phys. **104**, 7590 (1996).
[15] W. M. Huo and S. Green, J. Chem. Phys. **104**, 7572 (1996).
[16] For consistency with a master equation approach for distinguishable molecules, we prefer the notation $\sigma^e_{ij\to m\ell}$ for the exchange term in Eq. (3), instead of $\sigma^e_{ij\to \ell m}$ employed by W. M. Huo and S. Green in J. Chem. Phys. **104**, 7572 (1996).
[17] A. van der Avoird, P. E. S. Wormer, and A. P. J. Jansen, J. Chem. Phys. **84**, 1629 (1986).
[18] S. Green, J. Chem. Phys. **62**, 2271 (1975).
[19] J. M. Hutson and S. Green, MOLSCAT version 14, Collaborative Computational Project No. 6 of the UK Science and Engineering Research Council, 1994.
[20] D. Cappelletti, F. Vechiocattivi, F. Pirani, E. L. Heck, and A. S. Dickinson, Mol. Phys. **93**, 485 (1998).
[21] M. H. Alexander and D. E. Manolopoulos, J. Chem. Phys. **86**, 2044 (1987).
[22] K. Takayanagi, Adv. At. Mol. Phys. **1**, 149 (1965).
[23] See EPAPS Document No. E-JCPSA6-127-013737 for the file N2RATES.TXT with the close coupling calculated (down) rates for $N_2:N_2$ collisions between 2 and 50 K. This document can be reached through a direct link in the online article's HTML reference section or via the EPAPS homepage (http://www.aip.org/pubservs/epaps.html).
[24] B. Maté, F. Thibault, G. Tejeda, J. M. Fernández, and S. Montero, J. Chem. Phys. **122**, 064313 (2005).
[25] S. Montero, F. Thibault, G. Tejeda, and J. M. Fernández, J. Chem. Phys. **125**, 124301 (2006).
[26] G. Tejeda, B. Maté, J. M. Fernández-Sánchez, and S. Montero, Phys. Rev. Lett. **76**, 34 (1996).
[27] A. Ramos, B. Maté, G. Tejeda, J. M. Fernández, and S. Montero, Phys. Rev. E **62**, 4940 (2000).
[28] S. Montero, B. Maté, G. Tejeda, J. M. Fernández, and A. Ramos, in *Atomic and Molecular Beams: The State of the Art 2000*, edited by R. Campargue (Springer, Berlin, 2001), p. 295.
[29] H. Rabitz and S. Lam, J. Chem. Phys. **63**, 3532 (1975).

[30] L. K. Randeniya and M. A. Smith, J. Chem. Phys. **93**, 661 (1990).
[31] B. Maté, G. Tejeda, and S. Montero, J. Chem. Phys. **108**, 2676 (1998).
[32] D. Bermejo, P. Cancio, G. Di Lonardo, and L. Fusina, J. Chem. Phys. **108**, 7224 (1998).
[33] J. Doyle, B. Friedrich, R. V. Krems, and F. Masnou-Seeuws, Eur. Phys. J. D **31**, 149 (2004).
[34] T. Rieger, T. Junglen, S. A. Rangwala, G. Rempe, P. W. H. Pinkse, and J. Bulthuis, Phys. Rev. A **73**, 061402 (2006).